Fitness effects of *cis*-regulatory variants in the *Saccharomyces cerevisiae TDH3* promoter

Fabien Duveau[1], William Toubiana[2], and Patricia J. Wittkopp[1,3]

[1] Department of Ecology and Evolutionary Biology, University of Michigan, Ann Arbor, MI 48109 USA

[2] Institut de Génomique Fonctionnelle de Lyon, ENS de Lyon - CNRS UMR 5242 - Université Claude Bernard Lyon-1, 46 allée d'Italie, 69364 Lyon Cedex 07, France.

[3] Department of Molecular, Cellular, and Developmental Biology, University of Michigan, Ann Arbor, MI 48109 USA

Corresponding author:
Patricia J. Wittkopp
Department of Ecology and Evolutionary Biology
Department of Molecular, Cellular, and Developmental Biology
University of Michigan, Ann Arbor, MI 48109-1048 USA
wittkopp@umich.edu
Tel: +1.734.763.1548

Keywords: gene expression, distribution of mutational effects, robustness, fitness optimum, gene regulation

Abstract

Variation in gene expression is widespread within and between species, but fitness consequences of this variation are generally unknown. Here we use mutations in the *Saccharomyces cerevisiae TDH3* promoter to assess how changes in *TDH3* expression affect cell growth. From these data, we predict the fitness consequences of *de novo* mutations and natural polymorphisms in the *TDH3* promoter. Nearly all mutations and polymorphisms in the *TDH3* promoter were found to have no significant effect on fitness in the environment assayed, suggesting that the wild type allele of this promoter is robust to the effects of most new *cis*-regulatory mutations.

Main text

Genomic studies have identified extensive variation in gene expression within and between species (reviewed in Ranz and Machado 2006; Alvarez et al. 2015). Given the key role that gene expression plays in regulating development and physiology, many of these changes in expression are expected to affect higher order phenotypes, which may in turn affect fitness (reviewed in Gilad et al. 2006; Wray 2007; Carroll 2008; Fay and Wittkopp 2008; Wittkopp and Kalay 2012). Despite these often-stated expectations, only a handful of studies have directly measured the fitness effects of changes in gene expression (Dykhuizen et al. 1987; Perfeito et al. 2011; Rest et al. 2013; Keren et al. 2016), and most of these studies have used heterologous or synthetic promoters to alter gene expression level. It therefore remains largely unknown how differences in gene expression induced by new mutations in regulatory sequences relate to changes in organismal fitness. Here we use mutations in the promoter of the *TDH3* gene in *Saccharomyces cerevisiae* to alter *TDH3* expression levels and determine the impact of these expression changes on fitness during clonal growth in a rich medium containing glucose, which is the preferred carbon source for *S. cerevisiae* (Gancedo 1998). We then use this information to predict the fitness effects of new mutations and natural polymorphisms within the *TDH3* promoter that were previously characterized for their effects on expression (Metzger et al. 2015).

To alter *TDH3* expression levels, we selected eight mutations in the *TDH3* promoter (P_{TDH3}) that caused a broad range of changes in expression based on data from Metzger et al. (2015). The effects of these mutations on P_{TDH3} activity were determined in this prior study by inserting mutant alleles of the promoter upstream of a yellow fluorescent protein (YFP)

reporter gene and using fluorescence level as a proxy for TDH3 expression level (Metzger et al. 2015). We also analyzed (i) one strain with an un-mutated S288c wild type allele of P_{TDH3} driving expression of YFP, (ii) one strain with a null allele lacking the P_{TDH3}-*YFP* reporter gene, (iii) three strains with duplications of the reporter gene separated by a *URA3* marker and (iv) one strain with a *URA3* marker inserted downstream of the wild type P_{TDH3}-*YFP* reporter gene. The strains carrying a duplication of P_{TDH3}-*YFP* allowed us to examine increases in expression level and the URA3 marker strain served as a control for these duplication alleles. One of the duplication strains contained two copies of the wild type P_{TDH3} allele and the other two duplication strains carried a single point mutation in both copies of the promoter.

To quantify the impact of changing *TDH3* expression on fitness, each of these 14 P_{TDH3} alleles was independently introduced at the native *TDH3* locus, with duplications of the *TDH3* gene used to replicate effects on expression observed with the duplicated reporter gene. Prior work has shown that the effects of mutations in the P_{TDH3}-*YFP* reporter gene on fluorescence levels are nearly perfectly correlated ($R^2 > 0.99$) with the effects of the same mutations at the native *TDH3* locus measured using a TDH3-YFP fusion protein (Metzger et al. 2016). The fitness of these 14 strains was determined by co-culturing each strain with a common competitor strain in rich medium. Abundance of each strain relative to the competitor was quantified in at least eight replicates at four time points during ~21 generations of growth. Relative fitness was then calculated by dividing the fitness of each replicate population by the average fitness of the genotype carrying the wild type allele of P_{TDH3}. The expression level driven by the 14 P_{TDH3} alleles was estimated from the fluorescence level observed in the 14 corresponding reporter gene strains under the same conditions, with at least four replicates analyzed per strain. Relative fitness and median fluorescence (a proxy for gene expression level) of each genotype were then determined by averaging measures from the replicate populations.

These data allowed us to determine the relationship between *TDH3* expression level and fitness upon growth in rich medium. We found that a decrease in *TDH3* expression level as small as 6% relative to the wild type level significantly reduced fitness by 0.3% (*t*-test, t = -2.08, P = 0.045), while a 36% increase in expression level significantly decreased fitness by 1.0% (*t*-test, t = -10.70, P = 2.11×10^{-7}). No significant changes in fitness were observed for P_{TDH3} alleles driving expression levels between 96% (*t*-test, t = 1.67, P = 0.10) and 118% (*t*-

test, t =0.08, P = 0.94) of the wild type level (Figure 1), and none of the mutant alleles conferred a significantly higher fitness than the wild type *TDH3* promoter allele. Therefore, the relationship between *TDH3* expression and fitness in this environment includes a plateau of maximal fitness at expression levels ranging from 96% to 118% (at least) of the wild type expression level (Figure 1). 216 of the 235 (92%) mutations and 29 of the 30 (97%) natural polymorphisms previously characterized in the *TDH3* promoter (Metzger et al. 2015) resulted in expression levels included within this plateau of maximal fitness (Figure 1).

These observations suggest that changes in *TDH3* expression level generated by *cis*-regulatory mutations and polymorphisms in the *TDH3* promoter can be largely buffered at the fitness level. That is, the plateau near the fitness optimum appears to confer robustness of the wild type P_{TDH3} allele to most new *cis*-regulatory mutations, at least in the environment assayed. Non-linear fitness functions with plateaus located around the wild type level of expression have previously been described for the *LCB2* gene of *S. cerevisiae* using an inducible promoter (Rest et al. 2013) as well as for other yeast genes using synthetic promoters (Keren et al. 2016), and are consistent with predictions from metabolic flux control theory (Kacser and Burns 1973). These observations suggest that fitness plateaus might be common for expression-fitness curves and might play an important role in shaping the diversity of gene expression levels observed in natural populations.

Supplementary Materials

Supplementary Materials include (i) Supplementary Text with the Materials and Methods section, (ii) Supplementary Tables, including Table S1 (Position and nature of polymorphisms in the *TDH3* promoter) and Table S2 (List of oligonucleotides used to construct strains), Supplementary File 1 (Input tables for analyses of flow cytometry data), Supplementary File 2 (Output tables including all expression and fitness data), and Supplementary File 3 (R scripts used to analyze flow cytometry data).

Acknowledgements

We thank Chetna Gopinath for technical assistance, Brian Metzger, David Yuan, Bing Yang, and Andrea Hodgins-Davis for helpful discussions, and Brian Metzger, Jennifer Lachowiec, and Andrea Hodgins-Davis for comments on the manuscript. This work was supported by a European Molecular Biology Organization postdoctoral fellowship (EMBO ALTF 1114-2012)

to F.D., a Ph.D. fellowship from Ecole Doctorale BMIC de Lyon to W.T., and grants from the National Science Foundation (MCB-1021398) and National Institutes of Health (R01GM108826 and 1R35GM118073) to P.J.W.

References

Alvarez M, Schrey AW, Richards CL. 2015. Ten years of transcriptomics in wild populations: what have we learned about their ecology and evolution? Mol. Ecol. 24:710–725.

Carroll SB. 2008. Evo-devo and an expanding evolutionary synthesis: a genetic theory of morphological evolution. Cell 134:25–36.

Dykhuizen DE, Dean AM, Hartl DL. 1987. Metabolic flux and fitness. Genetics 115:25–31.

Fay JC, Wittkopp PJ. 2008. Evaluating the role of natural selection in the evolution of gene regulation. Heredity (Edinb) 100:191–199.

Gancedo JM. 1998. Yeast carbon catabolite repression. Microbiol. Mol. Biol. Rev. 62:334–361.

Gilad Y, Oshlack A, Rifkin SA. 2006. Natural selection on gene expression. Trends in Genetics 22:456–461.

Kacser H, Burns JA. 1973. The control of flux. Symp. Soc. Exp. Biol. 27:65–104.

Keren L, Hausser J, Lotan-Pompan M, Vainberg Slutskin I, Alisar H, Kaminski S, Weinberger A, Alon U, Milo R, Segal E. 2016. Massively Parallel Interrogation of the Effects of Gene Expression Levels on Fitness. Cell 166:1282–1294.e18.

Metzger BPH, Duveau F, Yuan DC, Tryban S, Yang B, Wittkopp PJ. 2016. Contrasting Frequencies and Effects of cis- and trans-Regulatory Mutations Affecting Gene Expression. Mol. Biol. Evol. 33:1131–1146.

Metzger BPH, Yuan DC, Gruber JD, Duveau F, Wittkopp PJ. 2015. Selection on noise constrains variation in a eukaryotic promoter. Nature 521:344–347.

Perfeito L, Ghozzi S, Berg J, Schnetz K, Lässig M. 2011. Nonlinear fitness landscape of a molecular pathway. PLoS Genet. 7:e1002160.

Ranz JM, Machado CA. 2006. Uncovering evolutionary patterns of gene expression using microarrays. Trends in Ecology & Evolution 21:29–37.

Rest JS, Morales CM, Waldron JB, Opulente DA, Fisher J, Moon S, Bullaughey K, Carey LB, Dedousis D. 2013. Nonlinear fitness consequences of variation in expression level of a eukaryotic gene. Mol. Biol. Evol. 30:448–456.

Wittkopp PJ, Kalay G. 2012. Cis-regulatory elements: molecular mechanisms and evolutionary processes underlying divergence. Nat Rev Genet 13:59–69.

Wray GA. 2007. The evolutionary significance of cis-regulatory mutations. Nat Rev Genet 8:206–216.

Figure 1. Fitness effects of *cis*-regulatory mutations and polymorphisms in the *TDH3* promoter.

The relationship between relative P_{TDH3} activity (as measured by fluorescence of a *YFP* reporter gene) and relative fitness is shown by the black points and the dotted curve. Each point represents the mean of median fluorescence levels (x-axis) among at least four replicate populations and the mean of relative fitness measurements (left y-axis) from at least seven replicate competition assays. Error bars show the 95% confidence intervals for both measurements. The relationship between P_{TDH3} activity and fitness (dotted curve) was defined using a LOESS regression of the fluorescence data on fitness. The greyed interval around the curve represents the 95% confidence interval of the LOESS regression, whereas the area shaded yellow indicates the range of *TDH3* expression levels with fitness comparable to the wild-type allele. Histograms showing the distributions of effects on P_{TDH3} activity (as measured by fluorescence of the same reporter gene) for 235 mutations (red) and 30 polymorphisms (blue) are overlaid on the fitness curve. Each bar represents a bin of 0.8% on the x-axis, and the number of mutants in each bin is shown on the right y-axis. The vertical and horizontal dotted lines show the fluorescence level and fitness conferred by the wild type *TDH3* promoter allele.

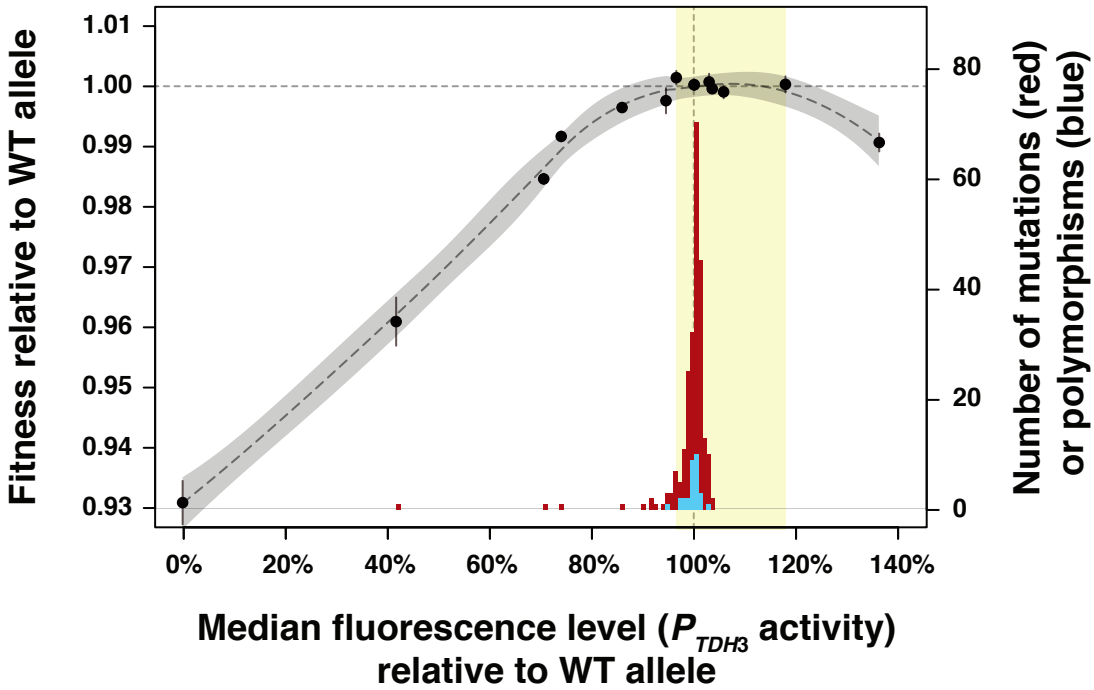
Fitness relative to WT allele
1.01
1.00
0.99
0.98
0.97
0.96
0.95
0.94
0.93
0%
20%
40%
60%
80%
100%
120%
140%
80
60
40
20
0
Number of mutations (red)
or polymorphisms (blue)
Median fluorescence level (P_{TDH3} activity)
relative to WT allele

Supplementary Materials for Duveau et al.: **"**Fitness effects of cis-regulatory variants in the Saccharomyces cerevisiae TDH3 promoter"

Materials and Methods

Strains used to quantify TDH3 promoter activity

The distributions of effects of mutations and polymorphisms on P_{TDH3} activity were described in (Metzger et al. 2015). In this previous study, 236 strains of *S. cerevisiae* were made in which each contained one of the 241 G:C to A:T base pair transitions in the 678bp *TDH3* promoter (P_{TDH3}) induced by site directed mutagenesis. These P_{TDH3} alleles were used to drive expression of a yellow fluorescent protein (YFP), with the entire P_{TDH3}-*YFP* reporter gene inserted near the *SWH1* pseudogene on chromosome 1 in the genetic background of the haploid *MAT**a*** strain BY4724 (Brachmann et al. 1998). One of these strains, m131, was excluded from this study because it appeared to have acquired a secondary mutation that affected fluorescence since data were collected for Metzger et al. (2015). Locations of the remaining 235 mutations are described in the Mutation.Positions worksheet in Supplementary File 1. 27 P_{TDH3} haplotypes observed among 85 strains of *S. cerevisiae*, containing a total of 45 different polymorphisms, were introduced upstream of the same reporter gene used to assess the effects of the point mutations. The evolutionary history of these P_{TDH3} haplotypes was inferred by comparing them to each other and to the homologous sequence from 15 distantly related strains of *S. cerevisiae* and from all *Saccharomyces sensu stricto* species. For pairs of haplotypes that differed by a single polymorphism, the effect of that polymorphism was inferred by comparing activity of the two haplotypes. For natural haplotypes that differed by two polymorphisms from their closest neighbor in the haplotype network, the effects of individual polymorphisms were determined by constructing intermediate haplotypes connecting natural haplotypes to their closest neighbor through single mutational steps. Natural haplotypes differing by more than two polymorphisms from all other haplotypes were excluded, reducing the number of unique polymorphisms from 45 to 30. In seven instances, the order of occurrence of two consecutive polymorphisms remained unresolved. In these cases, we calculated the effects of the two polymorphisms according to the two possible mutational paths (ab -> Ab -> AB and ab -> aB -> AB). A linear model was then applied to test for the significance of the interaction between the genotypes at the two

polymorphic sites on fluorescence levels. Among the seven pairs of polymorphisms tested, none of the interaction terms was significant ($P > 0.05$) after Bonferroni correction for multiple testing, although significant epistasis was detected for two pairs of polymorphisms without applying the multiple test correction ($P = 0.02$ and $P = 0.008$). We therefore averaged the effects of the polymorphisms quantified on the two possible mutational paths. Overall, this approach allowed us to estimate the effect of 30 individual polymorphisms in the promoter context where they most likely arose. A summary of variants present in each of the natural and inferred haplotypes is shown in Table S1, and the 45 pairs of haplotypes compared to infer the effects of 30 polymorphisms are shown in the Haplotype.Network worksheet of Supplementary File 1.

The 14 P_{TDH3} genotypes used to establish the relationship between TDH3 expression level and fitness are described in the Expression.vs.Fitness worksheet in Supplementary File 2. These genotypes were selected to cover a broad and homogenous range of promoter activity ranging from 0% to over 100%. To decrease the activity of the promoter, eight genotypes were chosen from the 235 strains constructed in Metzger et al. (2015) with single mutations in P_{TDH3}. The un-mutated progenitor strain of these lines, defined as the wild type allele of P_{TDH3}, was also included as the reference allele. As described in Metzger et al. (2015), our reference allele differs from the S288c P_{TDH3} sequence by a single base (G293a). The derived nucleotide is present in the 235 mutant alleles of P_{TDH3}, while the ancestral nucleotide is present in all natural and intermediate haplotypes. Because this single nucleotide difference was not found to interact epistatically with other mutations (Metzger et al. 2015), our relative measures of fluorescence (see below) correct for its effect on expression level. The original strain BY4724, which did not contain the P_{TDH3}-*YFP* reporter gene, was used to determine the baseline level of auto-fluorescence in cells when the promoter activity was effectively 0%. To increase expression of the YFP reporter gene, we created three strains with a duplication of the entire P_{TDH3}-*YFP* construct. One of these strains contained two copies of the wild type (S288c) *TDH3* promoter, while the other two strains carried a single mutation in each copy of the promoter (see Expression.vs.Fitness worksheet in Supplementary File 2). These duplications were created in a strain described in Metzger et al. (2016) that contains a few genetic differences from the strains characterized in Metzger et al. (2015). This haploid *MATα* strain contains alleles of *SAL1*, *CAT5* and *MIP1* that decrease the penetrance of the petite phenotype (Dimitrov et al. 2009), alleles of *RME1* and *TAO3* that

increase sporulation efficiency in diploids (Deutschbauer and Davis 2005), and has the P_{TDH3}-*YFP* construct inserted at the *HO* locus. We previously showed that mutations in P_{TDH3} had similar effects on the expression of the reporter gene in the two genetic backgrounds (Metzger et al. 2016). To create the different duplications, we first amplified by PCR each allele of the P_{TDH3}-*YFP* reporter gene with oligonucleotides 2687 and 1893 (Table S2) as well as the *URA3* cassette from the *pCORE-UH* plasmid (Stuckey et al. 2011) with oligonucleotides 2688 and 2686 (Table S2). Next, *URA3*-P_{TDH3}-*YFP* fusions were obtained using overlap extension PCR. These fusions were amplified by PCR with oligonucleotides 2684 and 2683 (Table S2) containing homology arms for insertion downstream of P_{TDH3}-*YFP* in strains carrying the reporter gene inserted at *HO* and with desired mutations in P_{TDH3} (Metzger et al. 2016). Therefore, the resulting strains carried a P_{TDH3}-*YFP*-*URA3*-P_{TDH3}-*YFP* duplicate reporter gene with the same allele of P_{TDH3} twice. For each strain, Sanger sequencing confirmed the correct sequence of the entire construct. Finally, to control for the effect of *URA3* on fluorescence level, we inserted the *URA3* cassette amplified with primers 2684 and 2685 (Table S2) downstream of P_{TDH3}-*YFP* in a strain carrying the wild type allele of P_{TDH3} at *HO.*

Quantifying P_{TDH3} activity by flow cytometry

For each strain, the median fluorescence level of at least 1500 cells was quantified by flow cytometry and used as a measure of the activity of the P_{TDH3} allele driving expression of *YFP* in that strain. The activity of the 235 P_{TDH3} alleles with single G:C to A:T transitions and the natural and intermediate haplotypes was previously assessed in nine replicate populations upon growth to saturation in rich medium (YPD) containing 10 g/L of yeast extract, 20 g/L of peptone and 20 g/L of dextrose (Metzger et al. 2015). We used here a similar approach to quantify the fluorescence levels of the three strains carrying duplication of the reporter gene and of the reference strain containing a single copy of the wild type reporter gene and the *URA3* marker. Each strain was revived from a frozen glycerol stock for 48 hours on medium lacking uracil (5 g/L ammonium sulfate, 1.7 g/L yeast nitrogen base, 1.44 g/L CSM-Ura, 3% v/v glycerol, 20 g/L agar) and then arrayed in eight replicate populations in 96-well plates containing 0.5 mL of YPD per well. After 22 hours of growth at 30°C, samples underwent three rounds of dilution to 2.5 x 10^4 cells/mL in fresh YPD followed by 12 hours of growth at 30°C. Then, cultures were diluted to 2.5 x 10^6 cells/mL in 96-well plates filled with 0.5 mL PBS per well. For each sample, the size and fluorescence level of more than 1000 individual

cells were quantified using a BD Accuri C6 flow cytometer coupled with a HyperCyt autosampler. A 530/30 nm optical filter was used to acquire the fluorescence emitted by YFP. This new dataset and the data collected in (Metzger et al. 2015) were all analyzed using custom R scripts (Supplementary File 3) similar to Metzger et al (2016). Briefly, events that did not correspond to single cells were filtered out using the clustering functions of the Bioconductor package *flowClust*. The relationship between forward scatter area (FSC.A) and forward scatter height (FSC.H) was then used to distinguish single cells, budding cells and pairs of cells. Non-fluorescent debris and dead cells were then removed, retaining only events corresponding to healthy fluorescent cells. The next step was to calculate a fluorescence level that did not depend on cell size. Indeed, the fluorescence intensity FL1.A is strongly correlated with FSC.A. To remove this correlation, we applied a principal component analysis on the logarithm of FSC.A and the logarithm of FL1.A for all filtered events. We then transformed the data following a rotation centered on the intersection between the two eigenvectors and of an angle defined by the first eigenvector and the vector between the origin and the intersection between the two eigenvectors. Transformed values of FL1.A were then divided by transformed values of FSC.A, yielding single cell fluorescence levels uncorrelated with FSC.A. For each sample, we then calculated the median fluorescence level of all cells and subtracted the auto-fluorescence measured from the strain without the reporter gene. Finally, the fluorescence signal of each sample was divided by the average fluorescence signal of the reference strain carrying the wild type allele of P_{TDH3} and averaged across replicates to obtain the relative fluorescence levels plotted on Figure 1.

Strains included in the fitness assays

To assess how changes in TDH3 expression level affected fitness, we introduced each of the 14 alleles of the *TDH3* promoter described in the Expression.vs.Fitness worksheet in Supplementary File 2 at the native *TDH3* locus. First, we created strain YPW1121 by replacing the native *TDH3* promoter with a *CORE-UK* cassette (Stuckey et al. 2011) amplified using oligonucleotides 1909 and 1910 (Table S2) in the *MAT***a** strain YPW1001 carrying the wild type allele of the P_{TDH3}-*YFP* reporter gene at *HO* (as well as a *NatMX4* drug resistance marker). YPW1001 genome also contained the alleles of *SAL1*, *CAT5* and *MIP1* decreasing petite frequency (Dimitrov et al. 2009) and the alleles of *RME1* and *TAO3* increasing sporulation efficiency (Deutschbauer and Davis 2005). For the non-duplicated alleles, we used genomic DNA from strains used in the fluorescence assays to amplify P_{TDH3} alleles

located upstream of *YFP* with oligonucleotides 2425 and 1305 (Table S2) specific to the insertion site on chromosome I and to the *YFP* coding sequence (to avoid amplification of the native *TDH3* promoter). The resulting PCR products were then amplified with 90 bp oligonucleotides 1914 and 1900 (Table S2) including 70 nucleotides of homology to the native *TDH3* locus at their 5' end. These products were then transformed in strain YPW1121 to replace the *CORE-UK* cassette with the mutated alleles of P_{TDH3}. Transformants were selected on 5-FOA plates and successful insertions of P_{TDH3} alleles were confirmed by Sanger sequencing. To determine fitness when *TDH3* expression level was 0%, we generated strain YPW1177 where the entire *TDH3* promoter and coding sequence were deleted. This was done by transforming strain YPW1121 with a PCR product obtained with primers 1345 and 1962 (Table S2) including homology to the sequences immediately upstream of the *TDH3* promoter and downstream of the *TDH3* stop codon. To quantify the fitness effects of increased *TDH3* expression level, we created three strains with duplication of the entire *TDH3* gene. In these strains, the alleles of the two copies of P_{TDH3} at the native locus correspond to the P_{TDH3} alleles present in the three strains with duplicated reporter genes (described in Expression.vs.Fitness worksheet in Supplementary File 2). First, we amplified with oligonucleotides 2687 and 1893 (Table S2) the *TDH3* promoter and coding sequence from the strains carrying at the native *TDH3* locus the three alleles to be duplicated. Then, the *URA3* cassette amplified from the *pCORE-UK* plasmid (Stuckey et al. 2011) with oligonucleotides 2688 and 2686 (Table S2) was fused to each *TDH3* amplicon by overlap extension PCR. The fusion products were amplified using oligonucleotides 2696 and 2693 (Table S2) with homology to *TDH3* 5'UTR and transformed in the genome of the three strains carrying the corresponding alleles of P_{TDH3} at the native locus. As a result, the structure of the *TDH3* locus after duplication was P_{TDH3}-*TDH3*-*URA3*-P_{TDH3}-*TDH3* with both copies of P_{TDH3} presenting the same allele. Correct sequences of the duplicated genes were confirmed by Sanger sequencing. Lastly, a strain was constructed by inserting the *URA3* cassette amplified with primers 2696 and 2697 (Table S2) downstream of *TDH3* in YPW1001 genome. This strain served as the wild type reference for measuring the fitness consequence of *TDH3* duplications by controlling for the impact of *URA3* expression on fitness. To measure the fitness of the 14 strains described above, each of them was grown for several generations in competition with the same competitor strain YPW1160. This strain expressed a *GFP* reporter gene so that it could be easily distinguished from the 14 strains expressing *YFP* using flow cytometry, as described below. To generate strain YPW1160, the *GFP* coding sequence

amplified using oligonucleotides 601 and 2049 (Table S2) was fused to the *KanMX4* drug resistance cassette amplified using oligonucleotides 2050 and 1890 (Table S2) using overlap extension PCR. The PCR product was then amplified with primers 601 and 1890 (Table S2) and transformed into strain YPW1001 to swap the *YFP-NatMX4* cassette at *HO* with *GFP-KanMX4*.

Quantifying fitness through competition assays

To precisely quantify the fitness of the 14 strains expressing *TDH3* under different alleles of the promoter, we used highly sensitive competition assays. First, starting from -80°C glycerol stocks, uracil auxotroph strains were revived on YPG plates (10 g/L yeast extract, 20 g/L peptone, 3% v/v glycerol, 20 g/L agar) and prototroph strains expressing URA3 were revived on plates lacking uracil (5 g/L ammonium sulfate, 1.7 g/L yeast nitrogen base, 1.44 g/L CSM-Ura, 3% v/v glycerol, 20 g/L agar). Then, the 10 [ura-] strains were arrayed in six 96-well plates containing 0.5 mL of YPD per well. Each plate contained 24 replicates of the reference strain, 24 replicates of a strain carrying a strong effect mutation in P_{TDH3} and 24 replicates of two other mutant strains (Layout.Fitness worksheet in Supplementary File 1). The four strains expressing URA3 (three strains with *TDH3* duplication and the corresponding reference strain) were arrayed in eight replicates on a separate plate that also contained other strains not included in this study (Layout.Fitness worksheet in Supplementary File 1). The fitness of these strains was measured in three separate experiments, with each experiment including a subset of the seven plates described above (Layout.Expression worksheet in Supplementary File 1). We also inoculated a matching set of 96-well plates for each experiment with only the GFP-expressing strain YPW1160 in every well. Plates were grown for 22 hours at 30°C on a roller drum to maintain cells in suspension. After growth, the optical density at 620 nm of all samples was recorded using a Sunrise plate reader, allowing us to calculate the average cell density for each plate. Using this information, we next mixed for each sample an approximately equal number of cells expressing YFP ([YFP+]) and of cells expressing GFP ([GFP+]) in clean plates. Then, an average of 4×10^4 mixed cells were diluted in 0.45 mL of fresh YPD medium so that the average cell density on each plate would reach approximately 5×10^6 cells/mL after 12 hours of growth at 30°C. After this initial phase of competitive growth, we performed two more rounds of cell density measurement, dilution to fresh YPD and growth for 12 hours so that all samples acclimated to constant growth in glucose. After this acclimation phase, the procedure of cell density measurement, dilution and growth was

repeated three more times, except that samples were grown for 10 hours between each dilution. After each dilution and also after the last round of growth, culture leftovers were diluted to 1.5 x 10^6 cells/mL in 0.3 mL of PBS in 96-well plates, placed on ice and run on the BD Accuri C6 flow cytometer. A 488 nm laser was used for excitation and the fluorescence emitted was acquired through two different optical filters at 510/15 nm and 585/40 nm, allowing separation of the GFP and YFP signals. At least 5,000 events were recorded for each sample at each of the four time points separated by 10 hours or ~7 generations of competitive growth (for a total of ~21 generations).

We then calculated the fitness of each population of [YFP+] cells based on the evolution of the ratio of [YFP+] by [GFP+] cells over time. To determine the frequency of [YFP+] and [GFP+] cells in each sample, we analyzed the flow cytometry data using custom R scripts (Supplementary File 3). After logarithmic transformation of raw data, we filtered out artifacts with extreme values of forward scatter (FSC.A and FSC.H) or fluorescence intensity (FL1.H acquired through the 510/15 filter and FL2.H acquired through the 585/40 filter). Two distinct populations could be distinguished based on FL2.H/FL1.H ratio. We fitted two normal curves to the distribution of FL2.H/FL1.H observed among all filtered events to distinguish events corresponding to [YFP+] cells (high value of FL2.H/FL1.H) and events corresponding to [GFP+] cells (low value of FL2.H/FL1.H). Using thresholds, we then counted the number of [YFP+] and [GFP+] cells analyzed by flow cytometry for each sample. Next, we calculated for each plate the number of generations of the reference strain between the four time points based on cell densities measured for the 24 wild type replicates at each time point and based on dilution factors. Finally, for each sample the number of generations calculated for the plate was regressed on the logarithm of the ratio of the number of [YFP+] cells divided by the number of [GFP+] cells using the R function *lm*. The exponential of the regression coefficient corresponded to the fitness of the [YFP+] population relative to the [GFP+] population (Hartl & Clark, 2007). We then divided the fitness of the 96 samples on each plate by the mean fitness of the 24 replicates of the reference strain on that plate, resulting in a measure of fitness expressed relative to the fitness of the reference strain (without mutation in the *TDH3* promoter). We used the *t.test* function in R for statistical comparison of the mean fitness of each strain to the mean fitness of the reference strain replicates present on the same plate.

Relationship between P_{TDH3} activity and fitness

To characterize the relationship between *TDH3* expression level and fitness, we performed a local regression (LOESS regression) of the mean fluorescence levels measured for the 14 strains expressing *YFP* under different alleles of P_{TDH3} on the mean fitness measured for the 14 strains expressing *TDH3* under the same P_{TDH3} alleles. We used the R function *loess* with a span of 0.8 to control the degree of smoothing.

Access to data and analysis scripts

Flow cytometry data used in this work is available through the Flow Repository (https://flowrepository.org): Repository ID = FR-FCM-ZZBN for data from Metzger et al. (2015) used to quantify the effects of 235 mutations and 30 polymorphisms in P_{TDH3} on expression, Repository ID = <pending> for data collected here to quantify the effects of duplications of the reporter gene on expression and Repository ID = <pending> for data collected here to quantify the fitness effects of 14 alleles of P_{TDH3}. The three R scripts used to perform the analyses described above ("Analysis of flow data for quantifying average fluorescence levels", "Analysis of flow data for quantifying fitness" and "Plot data shown on Figure 1") have been concatenated and provided as Supplementary File 3. Data tables used by these scripts are provided in Supplementary File 1. Specifically, Supplementary File 1 includes a description of each 96-well plate used to analyze expression (Layout.Expression.txt worksheet), a summary of the type of mutation (Mutation.Types.txt worksheet) and position of mutation (Mutation.Positions.txt worksheet) in each strain, a list of haplotypes compared to infer the effects of polymorphisms (Haplotype.Network.txt worksheet), a description of each 96-well plate used to analyze fitness (Layout.Fitness.txt worksheet), and measures used to convert optical density to cell density during fitness assays (Optical.Density.txt worksheet). The FCS files needed for each analysis must be placed in the same parent directory and must appear in the same order as in Layout.Expression.txt and Layout.Fitness.txt worksheets. Supplementary File 2 includes summary tables of expression and fitness for each genotype: a summary of strains, mutations, expression, and fitness used to plot the fitness function shown in Figure 1 (Expression.vs.Fitness worksheet), a summary of estimated expression level for the 235 mutations (Expression.Mutations worksheet), 45 haplotypes of P_{TDH3} (Expression.Haplotypes worksheet), 30 individual polymorphisms (Expression.Polymorphisms worksheet), and summaries of expression (Summary.Expression worksheet) and fitness (Summary.Fitness worksheet) in the format used by the script in Supplementary File 3 to produce Figure 1.

References

Brachmann CB, Davies A, Cost GJ, Caputo E, Li J, Hieter P, Boeke JD. 1998. Designer deletion strains derived from Saccharomyces cerevisiae S288C: a useful set of strains and plasmids for PCR-mediated gene disruption and other applications. Yeast 14:115–132.

Deutschbauer AM, Davis RW. 2005. Quantitative trait loci mapped to single-nucleotide resolution in yeast. Nat. Genet. 37:1333–1340.

Dimitrov LN, Brem RB, Kruglyak L, Gottschling DE. 2009. Polymorphisms in multiple genes contribute to the spontaneous mitochondrial genome instability of Saccharomyces cerevisiae S288C strains. Genetics 183:365–383.

Hartl DL, Clark AG. 2007. Principles of Population Genetics. 4th Edition. Sinauer Associates.

Metzger BPH, Duveau F, Yuan DC, Tryban S, Yang B, Wittkopp PJ. 2016. Contrasting Frequencies and Effects of cis- and trans-Regulatory Mutations Affecting Gene Expression. Mol. Biol. Evol. 33:1131–1146.

Metzger BPH, Yuan DC, Gruber JD, Duveau F, Wittkopp PJ. 2015. Selection on noise constrains variation in a eukaryotic promoter. Nature 521:344–347.

Stuckey S, Mukherjee K, Storici F. 2011. In vivo site-specific mutagenesis and gene collage using the delitto perfetto system in yeast Saccharomyces cerevisiae. Methods Mol. Biol. 745:173–191.

Supplementary Files and Tables

Supplementary Tables, including Table S1 (Position and nature of polymorphisms in the *TDH3* promoter) and Table S2 (List of oligonucleotides used to construct strains).

Supplementary File 1. Input tables for analyses of flow cytometry data.

Supplementary File 2. Output tables including all expression and fitness data.

Supplementary File 3. R scripts used to analyze flow cytometry data.